PAPER • OPEN ACCESS

Solution combustion synthesis of Mo-Fe/MgO: Influence of the fuel composition on the production of doped catalyst nanopowder

View the article online for updates and enhancements.

Solution combustion synthesis of Mo-Fe/MgO: Influence of the fuel composition on the production of doped catalyst nanopowder

R Y S Zampiva[1], C P Bergmann[1], A K Alves[1] and L Giorgini[2]

[1] Post-Graduation Program in Mining, Metallurgy and Materials Engineering (PPGE3M), Federal University of Rio Grande do Sul, Osvaldo Aranha 99, 90035-190, Porto Alegre, Brazil
[2] Department of Industrial Chemistry "Toso Montanari", University of Bologna, Viale del Risorgimento 4, 40136, Bologna, Italy

E-mail: rubiayoungsun@gmail.com

Abstract. Among the techniques for producing oxide catalysts, the solution combustion synthesis (SCS) has been widely used to produce high-quality nanostructured powders at low-cost. Through SCS, due to the high exothermic energy liberated by the reaction between the transition metal nitrate and the fuel, it is possible to homogeneously incorporate dopant ions into the catalyst. Besides, SCS allows the production of nanopowders with sizes in the decimal scale, which is extremely important for powdered catalysts. The smaller the particle is, the larger the surface area is. Based on these possibilities, the aim of this work is to produce Fe-Mo/MgO nanopowders by SCS. The influence of concentration and composition of the fuels glycine and polyethylene glycol (PEG) on the final product were investigated. The morphology and the physicochemical properties were characterized by X-ray diffraction (XRD), electron microscopy (SEM), granulometry and surface area analysis. The results indicated high crystallinity for the samples produced with PEG and a wide variation on the nanoparticles sizes depending on the fuel properties.

1. Introduction

Along the past few years, nanoscience has become a focus of research in several areas of development due to the different material properties evidenced in the nanometer scale [1-7]. For example, some materials when nanostructured are exceptionally strong, hard and ductile at high temperatures [8-9]. These characteristics are controlled by the size, composition and morphology of the material [10]. Among these nanomaterials a group that is attracting great interest is the nanostructured catalysts, sized between 1 and 100 nm. Such catalysts have high efficiency, because the surface of the particles have greater availability to carry out catalysis [11]. The smaller the particle diameter, the greater the number of atoms exposed on the surface. As the diameter, purity and homogeneity of the catalyst are of fundamental importance for the yield of the reactions in which it is employed [10]. Mo-Fe/MgO spinel is an excellent catalyst for multiwall carbon nanotubes production [11].

SCS technique has been increasingly applied in the production of oxides catalysts due to the possibility to produce, at low-cost, highly pure and homogeneous nanostructured powders. SCS consists basically of the combination of its reactants in an aqueous medium using a complexing agent

(fuel) [12] such as citric acid [13,14] ; oxalic acid; tetraformol trisazine [12], glycine [4], urea [15], among others, and oxidizing agents (usually metal nitrates), responsible for oxidizing the fuel. The mixture is heated between 150 °C and 500 °C in order to carry out a self-ignition that leads to a fast combustion reaction that can reach more than 1700 °C [16] forming at the end of the process a solid product usually crystalline and well dispersed [17].

The high exotherm resulting from the reaction between the transition metal nitrate and fuel allow the incorporation of dopant ions in the catalyst [18]. The distribution of dopants throughout the host material is uniform because of the atomic mixing of the reactants in the initial solution. The dopants may drastically alter the properties of the catalyst even if the concentration in the crystalline structure is very low (1-3% atom) [12]. The easily incorporation of dopant ions is important for the production of structures such as Fe-Mo/MgO, where MgO is the host for Fe and Mo catalyst ions. Fe-Mo/MgO is an important catalyst for the production of single and multiwall carbon nanotubes. The synthesis parameters strongly affect the produced catalyst activity [19].
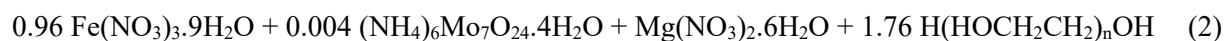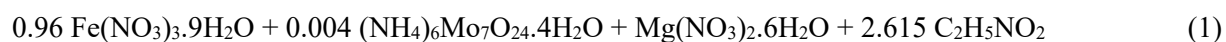
The stoichiometry of a combustion reaction is calculated through the chemistry of propellants [20] and it is generally expressed in terms of the equivalence ratio (Ø). An equivalence ratio of 1 signifies a stoichiometrically balanced combustion reaction, where the oxidizing power of the metal nitrates is equal to the reducing valence of the fuel. Positive departure (Ø>1) of the equivalence ratio signifies fuel-lean compositions, whereas negative departure (Ø<1) denotes fuel-rich compositions. Different products can be formed by varying the reducing potential of the precursor solution [21]. Furthermore, properties such as particle size, shape, morphology and agglomeration are directly influenced by the combustion conditions [22. 23].

Therefore, in this paper, in order to formulate the optimal methodology for preparing nanostructured oxides for catalysis, we studied the relationship of fuel-oxidant concentration, and the use of glycine and polyethylene glycol with molecular weight 200 (PEG) as fuel in the SCS of Fe-Mo/MgO nanopowder catalyst.

2. Materials and Methods

2.1. Synthesis of Fe-Mo/MgO

In order to produce Fe-Mo/MgO by SCS, iron nitrate nonahydrate ($Fe(NO_3)_3.9H_2O$), ammonium heptamolybdate tetrahydrate (($(NH_4)_6Mo_7O_{24}.4H_2O$) and magnesium nitrate hexahydrate ($Mg(NO_3)_2.6H_2O$) were used as ions precursors and oxidizing agents. The syntheses efficiency was studied varying the concentration of glycine ($C_2H_5NO_2$) and PEG 200 ($H(HOCH_2CH_2)nOH$) as fuel. All precursors were acquired from Sigma-Aldrich. The precursors concentration and the stoichiometric correlation for both fuels are indicated by Equations 1 and 2:

$$0.96\ Fe(NO_3)_3.9H_2O + 0.004\ (NH_4)_6Mo_7O_{24}.4H_2O + Mg(NO_3)_2.6H_2O + 2.615\ C_2H_5NO_2 \qquad (1)$$

$$0.96\ Fe(NO_3)_3.9H_2O + 0.004\ (NH_4)_6Mo_7O_{24}.4H_2O + Mg(NO_3)_2.6H_2O + 1.76\ H(HOCH_2CH_2)_nOH \quad (2)$$

Briefly explaining, through the propellants chemistry, the stoichiometric correlation between fuel-oxidizer is reached with the valences neutralization. N is considered neutral, while for the equations above, Fe presents a valence of +3, Mg of +2, Mo of +6, H of +1, O of -2 and C of -4. The fuel-oxidizer correlation is given by the equivalence ratio Ø, equation 3:

$$Ø = Oxidizer\ /\ Fuel \qquad (3)$$

When the sum of the oxidizer valences is equal to the sum of the fuel valences, the combustion reaction is considered stoichiometric (Ø = 1). Ø > 1 signifies fuel-lean compositions while (Ø<1) means fuel-rich compositions. Based on the stoichiometric combustions, rich and lean compositions were formulated in order to verify the influence of the fuel composition and concentration on the product. The samples were divided in glycine and PEG 200 groups and are described in Table 1:

Table 1. Composition and concentration of the fuels used to produce Fe-Mo/MgO by SCS.

Sample	Fuel	Ø	Description	Concentration (mol)
G1		0.66	Rich	3.975
G2	Glycine	1	Stoichiometric	2.615
G3		2	Lean	1.3
P1		0.665	Rich	0.855
P2	PEG	1	Stoichiometric	0.57
P3		1.995	Lean	0.285

The salts and fuels were individually dissolved in distilled water and then mixed (first the salts and then the specific fuel was added) in order to avoid precipitation during the solubilization processes. The solution was heated at 60°C during 5 min under constant stirring. This methodology was applied for all samples. After complete mixing, the samples were inserted in a 400 °C pre-heated electric muffle furnace during 15 minutes in order to undergo self-ignition. The samples were then calcined at 1100 °C in order to burn the carbonic residues and to organize the crystalline structure of the powdered product.

2.2. Characterization
The crystallinity of the samples was evaluated by X-ray diffraction (XRD) using a PHILIPS diffractometer (model X'Pert MPD) at 40 kV and 40 mA using a Cu anode. The particles surface area was obtained by the nitrogen adsorption method (BET - Quanta Chrome, Nova- 1000 model). As well the catalyst granulometric distribution was measured using a laser diffraction method in a Cilas-180L. the morphology of the Fe-Mo/MgO nanoparticles was characterized by scanning electron microscopy (SEM) using a JEOL microscope (JSM 6060) with a maximum operating voltage of 30 kV and a nominal resolution of 3.5 nm. The applied voltage was 10 to 20 kV. Transmission electron microscopy (TEM) was also carried out using a JEOL microscope (JEM 1200 EXII model) operating between 80 and 100 kV with a point resolution of 0.45 nm and line resolution of 0.20 nm. The powder sample was placed on a Cu grid and coated with a carbon film, to avoid magnetic interactions with the TEM microscope.

3. Results and discussion
According to diffractogram (figure 1), all samples produced using PEG present the characteristic peaks for periclase (MgO JCPDF # 00-001-1235, cubic Fm-3m) indicating the formation of MgO as host for Fe and Mo in the structure of Fe-Mo/MgO. It is possible to also observe a second phase that might be related to the formation of iron oxide. Interestingly, the fuel-lean combustion presented the purest composition among the PEG produced samples. The fuel concentration has a direct influence on the second phase formation; higher concentration leads to an ignition that reaches elevated temperature in really short time. The fast precipitation (crystallization) of the sample tends to produce nonstoichiometric or also heterogeneous samples, composed by more than one phase [24, 25]. The powders produced with glycine, did not presented the formation of the desired phases, indicating mostly the presence of amorphous phase. Since glycine did not show favourable results to produce Fe-Mo/MgO, the following analyses were performed only for PEG samples.
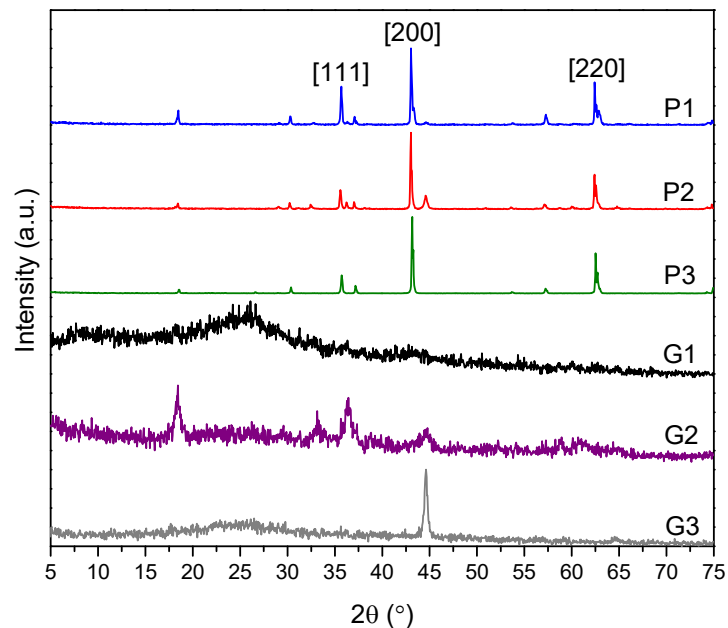
Figure 1. Samples diffractogram correlating the crystalline structure and SCS fuel concentration and composition. The peaks [111], [200] and [220] belong to periclase (MgO JCPDF # 00-001-1235, cubic Fm-3m).

Through the PEG micrograph is possible to observe that the particles morphology and diameter are very similar to all samples corroborating with the XRD analyses that also indicated a similar degree of crystallinity between samples. The elevated grain size (2 μm) might me related to the nanoparticles agglomeration tendency, leading to the formation of large grains, as observed in figure 2a, b and c.
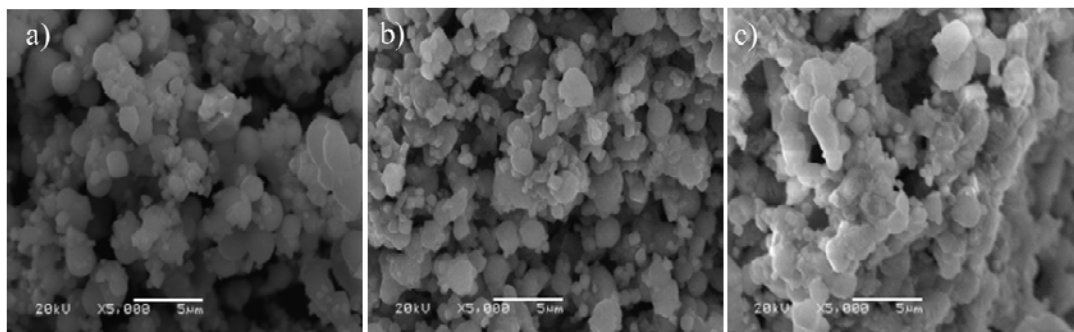

Figure 2. PEG samples SEM micrograph: a) P1, b) P2 e c) P3.

The granulometric results (figure 3) indicated different grain sizes for each composition. However, all samples are manly composed by large grains. The elevated diameters are in accordance with the micrograph analysis, indicating also here the agglomeration of nanoparticles. This phenomenon occurs guided by forces such as Van der Waals in direction to a lower energy state, reducing the interfaces with the environment [4].

Sample P2 presented the major concentration of nanoparticles (under 1 μm). Both samples P2 and P3 showed particles with a maximum size under 100 μm, while 30% of P1 is formed of particles around 100 and 1000 μm. P1 has the most agglomerated particles while P2 presented the higher dispersion, also indicated by the 20% of nanoparticles in the sample. To correctly analyze these results is important to considerate that no process of ultrasonification, sifting or milling was applied to the final product.
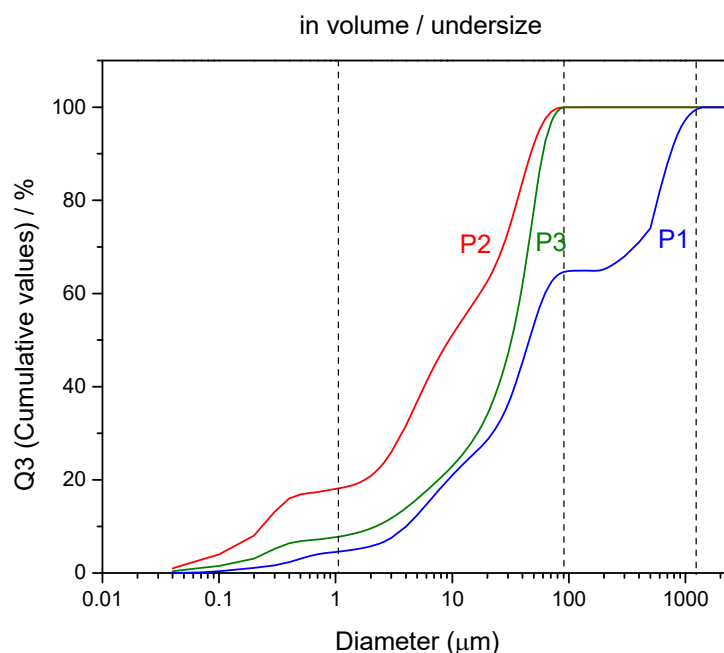
Figure 3. PEG samples granulometry.

Table 2 shows the surface area of the samples P1, P2 and P3. P3 presented the highest surface area among the samples: 29,712 m²/g followed by the stoichiometric sample P2 (27,757 m²/g). Indicating a higher degree of dispersion and also corroborating with the agglomeration theory discussed above. The smallest surface area was found for sample P1(10,3 m²/g) and is in accordance to the granulometry results that indicated the largest grains for this sample. The smaller the grains, the higher the surface area.

Table 2. Surface area of the samples P1, P2 and P3

Sample	Superficial Area (m²/g)
P1	10.292
P2	27.757
P3	29.712

Analyzing the table 2 is possible to infer that for the stoichiometric composition s not always the best choice for the production of nanostructured catalysts by SCS. The surface area is strongly dependent of the synthesis parameters, and the fuel concentration and composition directly alter the temperature, velocity and also the chemical composition during the crystal formation [4]. The influence of the fuel was also well observed through the XRD, granulometry and SEM analyses.

4. Conclusions

Nanostructured oxide catalysts were successfully obtained through the SCS method using PEG as fuel. The XRD analysis indicated that glycine was not efficient for the production of Fe-Me/MgO, presenting mostly an amorphous phase. All samples prepared with PEG showed elevated crystallinity and through the BET, granulometry and SEM analyses was possible to observe that the concentration of fuel strongly influences the properties of the final product. We conclude that not necessarily the stoichiometric formulation will be the best path to produce nanomaterials. For each final product, the precursors and fuels composition should be individually studied in order to choose the best combination of oxidizer/fuel composition and concentration. In the case of Fe-Mo/MgO catalyst, the best formulation was the PEG fuel-lean that presented the largest surface area among the samples.

Acknowledgement

References

[1]   Arcaro S, Wermuth T B, Zampiva R Y S, Venturini J, Caten C S, Bergmann C P, Alves A K, Oliveira A P N De and Moreno R 2019 Li2O-ZrO2-SiO2/Al2O3 nanostructured composites for microelectronics applications, *J. Eur. Ceram. Soc.* **39**(2-3) 491-498

[2]   Zampiva R Y S, Acauan L H, Venturini J, Garcia J A M, da Silva D S, Han Z, Kassab L R P, Wetter N U, Agarwal A, Alves A K and Bergmann C P 2018 Tunable green/red luminescence by infrared upconversion in biocompatible forsterite nanoparticles with high erbium doping uptake, *Opt. Mater. (Amst).* **76** 407-415

[3]   Venturini J, Zampiva R Y S, Piva D H, Piva R H, Cunha J B M da and Bergmann C P 2018 Conductivity dynamics of metallic-to-insulator transition near room temperature in normal spinel, *J. Mater. Chem. C* **6**(17) 4720–6

[4]   Zampiva R Y S, Kaufmann Junior C G, Pinto J S, Panta P C, Alves A K and Bergmann C P 2017 3D CNT macrostructure synthesis catalyzed by MgFe2O4 nanoparticles—A study of surface area and spinel inversion influence, *Appl. Surf. Sci.* **422** 321-330

[5]   Fotouhi M, Saghafi H, Brugo T, Minak G, Fragassa C, Zucchelli A and Ahmadi M 2017 Effect of PVDF nanofibers on the fracture behavior of composite laminates for high-speed woodworking machines, *P I Mech Eng C-J Mec* **231**(1) 31-43

[6]   Kaufmann C G, Zampiva R Y S, Bergmann C P, Alves A K, Mortari S R and Pavlovic A 2018 Production of multi-wall carbon nanotubes starting from a commercial graphite Pencil using an electric arc discharge in aqueous medium, *FME Trans.* **46**(2) 151-156

[7]   Zampiva R, Venturini J, Acauan L, Kaufmann C, dos Santos L, Alves A, Bergmann C and Caten C S ten 2018 The impact of the reaction atmosphere on the additive-free growth of Mg$_2$B$_2$O$_5$ nanorods *Ceram. Int.* **45**(5) 6228-35

[8]   Guaglianoni W C, Cunha M A, Bergmann C P, Fragassa C, Pavlovic A 2018 Synthesis, Characterization and Application by HVOF of a WCCoCr/NiCr Nanocomposite as Protective Coating Against Erosive Wear, *Tribology in Industry* **40**(3) 477-487

[9]   Fotouhi M, Fragassa C, Fotouhi S, Saghafi M, Minak G 2019 Damage Characterization of Nano-interleaved Woven CFRP Under Fatigue Loading, *Fibers* **7**(2) no. 13, doi:10.3390/fib7020013.

[10] Rao C N R, Müller A and Cheetham A K 2005 *The Chemistry of Nanomaterials: Synthesis, Properties and Applications*

[11] Dubey P, Choi S-K, Kim B and Lee C-J 2012 Synthesis of thin-multiwalled carbon nanotubes by Fe-Mo/MgO catalyst using sol-gel method, *Carbon Lett.* **13** 99–108

[12] Patil KC, Hegde M S and Aruna S T 2008 Chemistry of Nanocrystalline Oxide Materials, *Chemistry of Nanocrystalline Oxide Materials* (India: WORLD SCIENTIFIC) 362

[13] Liu Z, Bian J, Huang Y, Xu T, Wang X and Dai S 2017 Fabrication and characterization of mid-infrared emission of Pr 3+ doped selenide chalcogenide glasses and fibres, *RSC Adv.* **7** 41520–6

[14] Huang Y, Tang Y, Wang J and Chen Q 2006 Synthesis of MgFe2O4 nanocrystallites under mild conditions, *Mater. Chem. Phys.* **97** 394–7

[15] Satyanarayana L, Reddy K M and Manorama S V 2003 Nanosized spinel NiFe2O4: A novel material for the detection of liquefied petroleum gas in air, *Mater. Chem. Phys.* **82** 21–6

[16] Dinka P and Mukasyan A S 2005 In Situ Preparation of Oxide-Based Supported Catalysts by

Solution Combustion Synthesis, *J. Phys. Chem. B* **109** 21627–33

[17] Zampiva R Y S, Kaufmann C G, Alves A K and Bergmann C P 2018 Influence of the fuel composition and the fuel/oxidizer ratio on the combustion solution synthesis of MgFe2O4 catalyst nanoparticles, *FME Trans.* **46**(2) 157-164

[18] Dubey P, Choi S K, Choi J H, Shin D H and Lee C J 2010 High-Quality Thin-Multiwalled Carbon Nanotubes Synthesized by Fe-Mo/MgO Catalyst Based on a Sol–Gel Technique: Synthesis, Characterization, and Field Emission, *J. Nanosci. Nanotechnol.* **10** 3998–4006

[19] Panic S, Bajac B, Rakić S, Kukovecz, Kónya Z, Srdić V and Boskovic G 2017 Molybdenum anchoring effect in Fe–Mo/MgO catalyst for multiwalled carbon nanotube synthesis, *React. Kinet. Mech. Catal.* **122** 775–91

[20] Jain S R, Adiga K C and Pai Verneker V R 1981 A new approach to thermochemical calculations of condensed fuel-oxidizer mixtures, *Combust. Flame* **40** 71–9

[21] Hadke S, Kalimila M T, Rathkanthiwar S, Gour S, Sonkusare R and Ballal A 2015 Role of fuel and fuel-to-oxidizer ratio in combustion synthesis of nano-crystalline nickel oxide powders, *Ceram. Int.* **41** 14949–57

[22] Nasiri H, Bahrami Motlagh E, Vahdati Khaki J and Zebarjad S M 2012 Role of fuel/oxidizer ratio on the synthesis conditions of Cu-Al2O3nanocomposite prepared through solution combustion synthesis, *Mater. Res. Bull.* **47** 3676–80

[23] Sral O, Ianos R, Istratie R and Pa C 2016 *Solution combustion synthesis of strontium* 1150–7

[24] Jovanović R, Rašuo B, Stefanović P, Cvetinović D and Swiatkowski B 2013 Numerical investigation of pulverized coal jet flame characteristics under different oxy-fuel conditions, *Int. J. Heat Mass Transf.* **58** 654–62

[25] Effenberg, G., Ilyenko S . 2008 *Ternary Alloy Systems Phase Diagrams, Crystallographic and Thermo– dynamic Data* (Springer Berlin Heidelberg)